Structural Engineering and Mechanics, Vol. 27, No. 6 (2007) 741-771
DOI: http://dx.doi.org/10.12989/sem.2007.27.6.741

Direct design of partially prestressed concrete solid beams

A. S. Alnuaimi†

Department of Civil and Architectural Engineering, College of Engineering, Sultan Qaboos University, Muscat, Sultanate of Oman

(Received February 5, 2006, Accepted June 19, 2007)

Abstract. Tests were conducted on two partially pre-stressed concrete solid beams subjected to combined loading of bending, shear and torsion. The beams were designed using the Direct Design Method which is based on the Lower Bound Theorem of the Theory of Plasticity. Both beams were of 300×300 mm cross-section and 3.8 m length. The two main variables studied were the ratio of the maximum shear stress due to the twisting moment, to the shear stress arising from the shear force, which was varied between 0.69 and 3.04, and the ratio of the maximum twisting moment to the maximum bending moment which was varied between 0.26 and 1.19. The required reinforcement from the Direct Design Method was compared with requirements from the ACI and the BSI codes. It was found that, in the case of bending dominance, the required longitudinal reinforcements from all methods were close to each other while the BSI required much larger transverse reinforcement. In the case of torsion dominance, the BSI method required much larger longitudinal and transverse reinforcement than the both the ACI and the DDM methods. The difference in the transverse reinforcement is more pronounce. Experimental investigation showed good agreement between design and experimental failure loads of the beams designed using the Direct Design Method. Both beams failed within an acceptable range of the design loads and underwent ductile behaviour up to failure. The results indicate that the Direct Design Method can be successfully used to design partially prestressed concrete solid beams which cater for the combined effect of bending, shear and torsion loads.

Keywords: beams; direct design method; bending; torsion; shear; prestressed concrete; partially prestressed concrete; concrete structures.

1. Introduction

Partially prestressed concrete structures are usually reinforced with a combination of non-stressed and prestressed reinforcement. Unlike the situation for fully prestressed structures, fine cracks may develop under service loads. The present code design equations for these structures are largely based on experimental results which have led to continuous changes in the code. Calculation of reinforcement for each load type is done separately and the results are then summed algebraically. This leads to conservative design. For combined loading, several interaction theories based on ultimate strength criterion have been developed, but the major weakness of this approach lies in the fact that it does not present a general design procedure capable of being applied to design for a

† Associate Professor, Ph.D., Corresponding author, E-mail: alnuaimi@squ.edu.om

given general stress state. Less effort has been directed in design towards applying the already accepted theories of mechanics.

Seraj *et al*. (1993) criticised the institutional codes for using design methods based on the truss analogy because of the unsatisfactory nature of the shear design provisions. They proposed an alternative, the 'Compressive-Force Path CFP' method for the design of reinforced and prestressed beams. They claimed that their method gives an adequate and rational explanation of the behaviour of structural concrete. They described their method as economic and safer design solution. However, the design equations they used, involved many empirical values which leaves the method vulnerable to changes and far from sound theoretical principles.

Wafa *et al*. (1995) used several methods for prediction of the torsional strength of pre-stressed concrete beams. They concluded that all methods used (i.e., the space truss with softening concrete, the space truss with spalling of concrete cover, and the skew bending) underestimated the torsional stiffness of all test beams. According to their study, among the methods used, the space truss theory with softening of concrete gave the best estimate of the torsional strength of the test beams.

Cohn and Lounis (1993) illustrated the contradictory standard recommendations on full pre-stressing and full inelastic redistribution of moment. They presented a design approach for partially prestressed structures as an extension to their earlier method for reinforced structures. The method was based on the equilibrium-serviceability method which satisfies the ultimate limit state of structural collapse and serviceability limit state criteria. In addition, the method imposes upper bounds on the permissible moment redistribution. The aim was to present a practical design approach to non-linear design for prestressed concrete structures.

Rahal (2001) and Rahal and Collins (1996, 2003a) criticized the ACI-318 (2002), the AASHTO-LRFD (1998) and Canadian CSA-A23.3 (1994) codes for not accounting for additional compression component caused by bending moment and not suitable for design and analysis of sections subjected to all of the stress resultants. They presented a simple model and simplified method for design and analysis of reinforced and prestressed beams for resisting torsion or both torsion and bending combined. They compared the results predicted by their models with results from experimental tests.

Hsu (1997) presented a background to the modification which appeared in the 1995 ACI building Code for design to resist shear and torsion. However, the empirical design equations presented in 1995 ACI code and considered to be rational, general and applicable to closed cross-sections of arbitrary shapes, have been changed in the 2002 ACI code especially those related to shear and torsion.

Karayannis and Chalioris (2000) employed a bilinear stress-strain relationship with a post cracking tension softening branch for analysis and prediction of the ultimate strength of prestressed concrete beams under torsion and torsion combined with shear and flexure. They compared results given by their analytical model with the experimental results and code provisions. The model was mainly applied to plain pre-stressed element or pre-stressed concrete beams with light transverse reinforcement. The interaction curves used included empirical values

Poulsen and Damkilde (2000) used the lower bound theorem of the theory of plasticity for the analysis of reinforced concrete plates subjected to in-plane forces.

Aguilar *et al*. (2002) in their support for proposed modification of the ACI318 code stated: "the shear designs of the deep beams tested using the ACI318-99 code and Appendix A of the ACI318-02 were shown to be conservative". They deemed the 25% degree of conservatism observed in some of the tested specimens as appropriate at this time until more experimental

information is available.

Rahal and Collins (2003b) carried out experimental investigation in order to evaluate the ACI and AASHTO-LRFD design provisions for combined torsion and shear. They found that the ACI provisions give very conservative results if the recommended value of 45-degree is used for the inclination of the compression diagonals.

Zia and Hsu (2004) presented what they call "a unified method for torsion and shear design of prestressed and non-prestressed concrete flexural members". They claim that this method provides an alternative to the provision of the ACI building code (2002) and it forms the basis for shear and torsion provisions in the Sixth Edition of the PCI Design Handbook (2004). The aim was to produce simple and reliable design equations as an alternative to the institutional codes.

Recupero *et al*. (2005) presented an analytical model for the axial force-bending moment-shear force interaction, based on the stress field approach which includes the effect of pre-stressing tendons. They claimed that their model provides a unified approach for reinforced and pre-stressed concrete. They tested their model against experimental results and found that it gives a lower bound solution.

It is clear from the above literature and others that large number of researchers are not satisfied with the existing equations used for design in the codes of practice and therefore searching for a widely accepted methods especially in the case of loads combining bending, shear and torsion. One reason for this dissatisfaction is the fact that the design equations used in the code are not based on sound theoretical principles such as the theories of mechanics (i.e., Theory of Plasticity). Involvement of empirical values and values for the contribution made by concrete in the design equations, lack of sufficient research data and contradicting results can be detected in the existing design methods accepted by the codes. Many researchers described their models as general, rational and unified, but modified them based on new findings. Even those who criticised the codes for being conservative have used empirical values in their design equations (i.e., Rahal and Collins (2003b)).

The Direct Design Method, which is based on the Lower Bound Theorem of the Theory of Plasticity, presents a solution to some of the design code pitfalls. This procedure satisfies the fundamental requirements of the classical Theory of Plasticity (equilibrium condition, yield criterion and mechanism condition) and it reduces the ductility demand assumed for metals as explained in sections 3 and 4 below. In contrast to the existing codes of practice, this method precludes the use of empirical equations and therefore, is less vulnerable to changes and may form the basis for a unified design method.

The direct design method has been successfully used for the design of different structures (Memon (1984), Abdel-Hafez (1986), Hago and Bhatt (1986), Bhatt and Ebireri (1989), Bhatt and Bensalem (1996a, b), Bhatt and Mousa (1996), Alnuaimi and Bhatt (2004a,b), Alnuaimi and Bhatt (2006a,b), Alnuaimi *et al*. (2007a,b)). More information about the direct design method can be found in the literature (El-Hussein (1994), Elarabi (1999), Kemp (1971), Morley and Gulvanessian (1977), Nielsen (1974), Nielsen (1985), Clark (1976)).

In this research, the direct design method was used for the design of two partially pre-stressed concrete solid beams. The aim was to study the effects, on the beam behaviour and ultimate load, of varying the ratio of the shear stress due to torsion to the shear stress due to shear force and the ratio of twisting moment to bending moment.

2. Research significance

A general procedure for the design of partially prestressed concrete solid beams subjected to combined bending, torsion and shear loading is presented. The effects of varying the ratios between torsion induced and shear force induced shear stresses and torsion and bending moments on the beam behaviour and ultimate load are presented. The required reinforcement in each beam is compared with the requirements of the ACI and the BSI codes.

3. Stresses and direct design

It is well known that most of the torsion is resisted by the outer shell of the solid section and the core participation is minimal while the direct shear stress is uniformly distributed across the whole width of the cross-section with a parabolic shape through the height with minimal stress in the top and bottom strips and maximum at mid-depth. The thickness of the wall resisting torsion in a solid member was estimated to be in the order of one-sixth to one-quarter of the minimum width of a rectangular member (i.e., Hsu (1968), Thulimann (1979), Mitchell and Collins (1991), Rahal and Collins (1995), MacGregor and Ghoneim (1995), Alnuaimi and Bhatt (2006b).

The main stress conditions in the solid partially pre-stressed concrete beams, due to the combined torsion, bending, shear and axial force, loading are the direct stresses as shown in Fig. 1. The forces involved in out-of-plane bending are very small and can be ignored. If the direct shear stresses at the top and bottom strips are ignored, then at any point in the cross-section, a biaxial state of stress is maintained as shown in Fig. 2. This suggests that a plane stress distribution at any point in the cross-section and the design equations derived by Nielsen (1974, 1985) for in-plane forces, based on the yield criterion given in Eq. (1), can be used for the design of solid partially pre-stressed beams.

$$(N_x^s - N_x)(N_y^s - N_y) - N_{xy}^2 = 0 \tag{1}$$

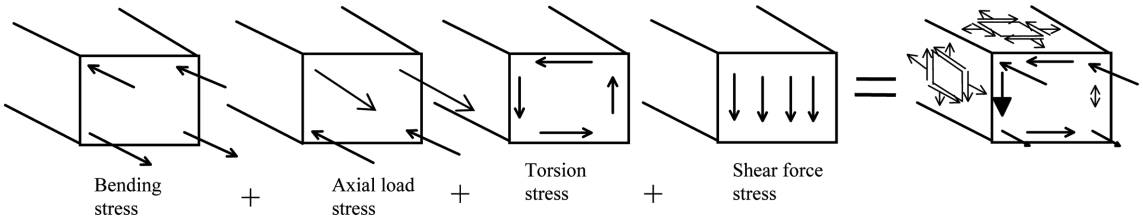

Fig. 1 Stresses in a solid section due to applied loads

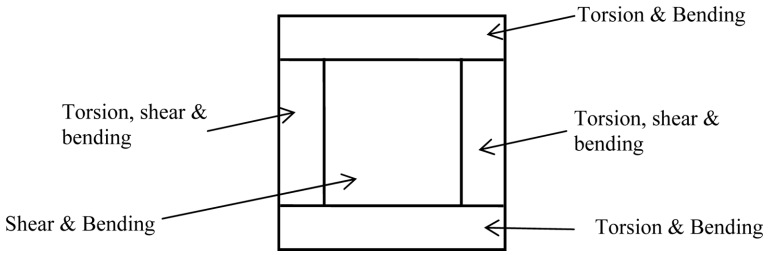

Fig. 2 Assumed biaxial state of stress across the beam section

At the top and bottom strips, net normal stress due to bending and the axial force is combined with the shear stress due to torsion. This biaxial stress can be used to calculate the required longitudinal and transverse reinforcement for these strips. Similarly, in the middle section, the net normal stress due to bending and the axial force is combined with the shear stress due to the shear force. This can be used to calculate the required longitudinal and transverse reinforcement in this section. Finally, in the vertical strips, the net normal stress due to bending and axial load combined with the net shear stress from torsion and shear force are used to calculate the required longitudinal and transverse reinforcement in these strips.

The yield criterion in Eq. (1) and the design equations proposed by Nielsen (See the example in appendix A) satisfy the ultimate limit state design as follows:

1. For each point in the structure calculate a set of stress in equilibrium with the external loads. The stress distribution can be derived from elastic, plastic or any analysis as long as it is in equilibrium with the external loads. For ease, the elastic stress distribution was used in this research.
2. Calculate the required steel areas using Nielsen's equations. Stresses will not violate the yield criterion of the material because the yield criterion has been used to determine the steel areas.
3. Under ultimate load, the structure will develop sufficient plastic hinges to transform it into a mechanism because the resisting forces at hinges exactly balance the applied loads and therefore, theoretically, all points of the structure will yield simultaneously. In practice, however, this is not possible because it is difficult to provide exactly the required reinforcement for each point in the structure.

Unfortunately the theory of plasticity assumes unlimited material ductility. This means that the regions in the structure which yield early need to continue to deform without any reduction in their strength. Obviously, this is not the case with reinforced concrete and even less so with pre-stressed concrete. The direct design method, reduces the ductility demand made by the theory of plasticity because of the 'simultaneous' yielding of all points in the structure as in point 3 above. In other words the difference between the first yield load and ultimate load will be as small as practicable.

This procedure is called the Direct Design Method because the area of reinforcement is directly calculated from the stress field using Nielsen's equations.

In this research, the following was implemented in sequence:

1. The required reinforcements using the direct design method, the ACI code and the BSI code for the same load combinations, beam geometry and material properties were calculated.
2. Comparison between the required reinforcement from the three methods was made.
3. Experimental investigation was carried out on two partially pre-stressed beams designed using the direct design method.

4. Direct design procedure

The following steps were used for the design of the partially prestressed concrete solid beams tested in this research and a numerical example with the design equations are given in appendix A. The concept of the method and detailed derivation of the design equations can be found in Alnuaimi and Bhatt (2004a, 2004b).

1. Calculate the ultimate design bending moment M_d, shear force V_d and torsion T_d at the section used for the design based on the loading condition, support locations and geometry of the beam.
2. Divide the cross-section into different cells (see the example in Appendix A).

3. Find the neutral axis, the second moment of area, I, and the area enclosed by the shear flow centreline.
4. Calculate normal stresses due to direct pre-stressing forces.
5. Calculate normal stresses due to eccentricities.
6. Add the stresses from steps 4 and 5. Check that the tensile stress in the upper extreme fibre is not exceeding the allowable tensile stress in the concrete.
7. Calculate the normal stress σ_{xb} due to the applied bending moment at the centre of each cell using the elastic stress distribution.
8. Calculate the net (design) normal stresses at service loads by algebraically summing all normal stresses. Check that the compressive stress in the top fibre is not exceeding the allowable compressive stress.
9. Calculate the shear stress in each cell due to shear force.
10. Calculate the shear stresses due to torsion.
11. Add the shear stresses to obtain the design shear stress for each cell.
12. Calculate the ratio of the normal stress to the shear stress.
13. Based on step 12 select the design case and equations as explained in the numerical example in appendix A.
14. Calculate the required longitudinal and transverse reinforcement.

5. ACI code procedure

When using the ACI 318M-02, Metric version, the following equations were used without material reduction factors:

1. Using the pre-stressing wires alone, the depth of the bending stress block was first calculated using Eq. (2)

$$a = \frac{A_{sp} f_{py}}{\phi f_c' b} \qquad \text{with} \qquad \phi = 0.85 \tag{2}$$

2. The bending moment of resistance of section when pre-stressing wires alone was calculated using Eq. (3)

$$\phi M_n = \phi A_{sp} f_{py} Z_p \qquad \text{with} \qquad \phi = 1 \tag{3}$$

3. Additional longitudinal bars for bending was calculated using Eq. (4)

$$(A_s)_{ben} = \frac{M_d - \phi M_n}{\phi f_y Z} \qquad \text{with} \qquad \phi = 1 \tag{4}$$

4. The new depth of the rectangular block was calculated using Eq. (5)

$$a = \frac{A_{sp} f_{py} + (A_s)_{ben} f_y}{\phi f_y' b} \qquad \text{with} \qquad \phi = 0.85 \tag{5}$$

5. The new bending moment of resistance including the pre-stressing wires and the normal longitudinal bars was calculated using Eq. (6)

$$\phi M_n = \phi [A_{sp} f_{ps} Z_p + (A_s)_{ben} f_y Z] \qquad \text{with} \qquad \phi = 1 \tag{6}$$

This trial an error method is repeated until the bending moment of resistance is almost equal to the applied bending moment.

6. To evaluate the shear force effect Eq. (7) with the conditions set in section ACI-11.4.1 was used.

$$V_c = \left(\frac{\sqrt{f_c'}}{20} + 5\frac{V_d d}{M_d}\right) b d \tag{7}$$

Provided $0.4\sqrt{f_c'}\, b d \geq V_c \geq \frac{\sqrt{f_c'}\, b d}{6}$ and $\frac{V_d d}{M_d} \leq 1.0$ where $\frac{V_d d}{M_d}$ = distance from extreme compression fibre to centroid of pre-stressed reinforcement.

7. Accordingly, the required reinforcement for direct shear, $(A_{sv}/S)_{shr}$, was calculated as stated in section ACI-11.5 using the appropriate equation.
8. Eq. (8) was used to evaluate the section adequacy for torsion (ACI section 11.6.3.1)

$$\sqrt{\left(\frac{V_d}{b d}\right)^2 + \left(\frac{T_d p_h}{1.7 A_{oh}^2}\right)^2} \leq \phi\left(\frac{V_c}{b d} + \frac{2}{3}\sqrt{f_c'}\right) \qquad \text{with} \qquad \phi = 1 \tag{8}$$

9. To evaluate the torsion effect Eq. (9) and the conditions set in section ACI-11.6.1 were used

$$T_d < \frac{\phi\sqrt{f_c'}}{12}\left(\frac{A_{cp}^2}{p_{cp}}\right)\sqrt{1 + \frac{3 f_{pc}}{\sqrt{f_c'}}} \qquad \text{with} \qquad \phi = 1 \tag{9}$$

10. Eq. (10) was used for the calculation of the transverse reinforcement for torsion with θ equal to 37.5° as recommended for pre-stressed members in the ACI-11.6.3.6.

$$\left(\frac{A_{sv}}{S}\right)_{tor} = \frac{T_d}{\phi 2 A_o \cot\theta} \qquad \text{with} \qquad \theta = 37.5^{\circ} \quad \text{and} \quad \phi = 1 \tag{10}$$

11. Eq. (11) was used for the calculation of the longitudinal reinforcement for torsion.

$$(A_s)_{tor} = \left(\frac{A_{sv}}{S}\right)_{tor} p_h \left(\frac{f_{yv}}{f_{yt}}\right)\cot^2\theta \qquad \text{with} \qquad \theta = 37.5^{\circ} \tag{11}$$

12. Eq. (12) was used for the calculation of the total transverse reinforcement for direct shear and torsional shear

$$\left(\frac{A_{sv}}{S}\right) = \left(\frac{A_{sv}}{S}\right)_{shr} + 2\left(\frac{A_{sv}}{S}\right)_{tor} \tag{12}$$

13. The longitudinal reinforcement for bending was added to that for torsion (Eq. (13)) to give the total required longitudinal reinforcement in addition to the area of the pre-stressing wires

$$A_s = (A_s)_{ben} + (A_s)_{tor} \tag{13}$$

6. BSI code procedure

When using the BSI8110-97 code the following equations were used without material reduction factors:

1. Using the pre-stressing wires alone the depth of the bending stress block was first calculated using Eq. (14)

$$a = \frac{A_{sp} f_{py}}{\lambda f_{cu} b} \qquad \text{with} \qquad \lambda = 0.67 \tag{14}$$

2. The moment of resistance with pre-stressing wires alone was calculated using Eq. (15).

$$MR1 = \psi[A_{sp} f_{py} Z_p] \qquad \text{with} \qquad \psi = 1 \tag{15}$$

3. Additional area of longitudinal bars for bending was calculated using Eq. (16)

$$(As)_{ben} = \frac{M_d - MR1}{\psi f_y Z} \qquad \text{with} \qquad \psi = 1 \tag{16}$$

4. The new depth of the rectangular block was calculated using Eq. (17)

$$a = \frac{A_{sp} f_{py} + (A_s)_{ben} f_y}{\lambda f_{cu} b} \qquad \text{with} \qquad \lambda = 0.67 \tag{17}$$

5. The new moment of resistance including the pre-stressing wires and the normal longitudinal bars was calculated using Eq. (18)

$$MR2 = \psi[A_{sp} f_{py} Z_p + (A_s)_{ben} f_y Z] \qquad \text{with} \qquad \psi = 1 \tag{18}$$

This trial an error method is repeated until the moment of resistance is almost equal the applied moment.

6. The applied torsional shear stress was calculated using Eq. (19)

$$v_{tor} = \frac{2T_d}{h_{\min}^2 (h_{\max} - h_{\min}/3)} \tag{19}$$

7. The direct shear stress was calculated using Eq. (20)

$$v_{shr} = \frac{V_d}{bd} \tag{20}$$

8. The total applied shear stress was calculated using Eq. (21)

$$v = v_{tor} + v_{shr} \tag{21}$$

9. The value of v from Eq. (21) was checked against the BSI8110-97 code values
$(v_t)_{\min} = 0.067\sqrt{f_{cu}}$ but not more than 0.4 N/mm^2.
$(v_{tu})_{\max} = 0.8\sqrt{f_{cu}}$ but not more than 5 N/mm^2.
When $v \geq (v_t)_{\min}$ transverse reinforcement for torsion should be provided and when $v \geq (v_{tu})_{\max}$ the section is to be resized.

10. The area of stirrups required for torsion was calculated using Eq. (22)

$$\left(\frac{A_{sv}}{S}\right)_{tor} = \frac{T_d}{0.8 x_1 y_1 (\psi f_{yt})} \qquad \text{with} \qquad \psi = 1 \tag{22}$$

11. The longitudinal steel for torsion was calculated using Eq. (23)

$$(A_s)_{tor} = \left(\frac{A_{sv}}{S}\right)_{tor}\left(\frac{f_{yt}}{f_y}\right)(x_1 + y_1) \tag{23}$$

12. Total area for longitudinal bars for torsion and bending was calculated using Eq. (24)

$$A_s = (A_s)_{ben.} + (A_s)_{tor.} \tag{24}$$

13. The un-cracked shear resistance was calculated using Eq. (25)

$$V_{co} = 0.67bh(\sqrt{f_t^2} + 0.8f_{cp}f_t) \tag{25}$$

14. The cracked section shear resistance was calculated using Eq. (26)

$$V_{cr} = \left(1 - 055\frac{f_{pe}}{f_{pu}}\right)v_c b d + M_o\frac{V_d}{M_d} \tag{26}$$

Where v_c was taken from Table 3.8 of the BSI code and M_o was calculated using Eq. (27)

$$M_o = \frac{0.8f_{pt}I}{y} \tag{27}$$

15. Since the tendons are straight, the value of concrete shear resistance V_c was taken to be the lesser of V_{co} and V_{cr}.
16. Accordingly Table 3.16 of the BSI was used for appropriate shear reinforcement $(A_{sv}/S)_{shr}$.
17. The total stirrup area was calculated using Eq. (28)

$$\left(\frac{A_{sv}}{S}\right) = \left(\frac{A_{sv}}{S}\right)_{tor} + \left(\frac{A_{sv}}{S}\right)_{shr} \tag{28}$$

7. Comparison between the ACI and BSI codes and the direct design method

In this research, two partially pre-stressed concrete beams, PPS1 and PPS2, were designed for different load combinations of bending moment, torsion and shear force as shown in Table 1. The beam cross-section was 300 × 300 mm and the length was 3.8 m. The beam loading and support arrangement are given in section 8. For pre-stressing, four 5 mm diameter wires were used in two locations. The eccentricity for the first pair was e_1 = 125 mm and for the second pair was e_2 = 75 mm. Each wire was stressed to a net force of P = 20 kN after losses. The ultimate strength of the pre-stressing wires f_{pu} was 1670 N/mm^2, the yield strength of the wires f_{py} was 1570 N/mm^2 and effective stress after losses was f_{pe} = 1018.6 N/mm^2. The concrete cube compressive strength was

Table 1 Load combinations and ratios

Beam No.	T_d	M_d	V_d	τ_{tor}	τ_{shr}	τ_{tor}/τ_{shr}	T_d/M_d
	kN·m	kN·m	kN	N/mm²	N/mm²	Ratio	Ratio
PPS1	13	50.89	61.08	2.08	3.00	0.69	0.26
PPS2	39	32.89	41.08	6.24	2.05	3.04	1.19

Table 2 Required reinforcement of unstressed bars using the ACI, BSI and DDM methods (with no reduction in material strengths)

Beam No.	ACI		BSI		DDM	
	A_s (mm^2)	A_{sv} (mm^2/m)	A_s (mm^2)	A_{sv} (mm^2/m)	A_s (mm^2)	A_{sv} (mm^2/m)
PPS1	332	332	425	760	383	505
PPS2	512	972	810	1800	490	1262

52 N/mm^2, the cylinder compressive strength was 36 N/mm^2 and the yield strength of the longitudinal and transverse reinforcing bars was 500 N/mm^2. The beams were designed using the ACI-318M (2002) and BSI (1997) codes and the direct design method DDM as described above. Table 2 shows the required reinforcement from the three procedures with material reduction factors being made equal to 1 as shown in the equations above. The values shown in this table are for reinforcing bars in addition to the partially pre-stressed wires which are not included in this table.

It is clear from Table 2 that with bending dominant case, PPS1, the required longitudinal reinforcement from all methods were close to each other with the ACI being the smallest and the BSI being the largest. However, the BSI required much larger transverse reinforcement than both the ACI and DDM. In the case of torsion dominance, PPS2, the BSI method required much larger longitudinal and transverse reinforcement than the both the ACI and the DDM methods. The difference in the transverse reinforcement is more pronounce.

Since the Direct Design Method is based on a sound theoretical principles (The Theory of Plasticity), less vulnerable to changes, systematic and can be easily programmed using any spread sheet program it was used for the design of the two partially pre-stressed beams tested in this research.

8. Experimental investigation

8.1 Tested beams

Two partially pre-stressed concrete solid beams were designed to allow for the combined action of bending, torsion and shear force (Table 1) using the Direct Design Method. Both beams had overall cross-sectional dimensions of 300 × 300 mm and 3.8 m length. The main variables studied were the ratio of the design shear stress at mid-depth due to the twisting moment and the shear stress due shear force τ_{tor}/τ_{shr} which was varied between 0.69 and 3.04 and the ratio of the design twisting moment to the bending moment T_d/M_d which was varied between 0.26 and 1.19.

8.2 Material used and beam construction

Rapid Hardening Portland Cement, 10 mm uncrushed gravel and sand were used in the concrete mix, prestressing wires were used to produce the axial force while high yield deformed bars were used for longitudinal and transverse reinforcement. Fig. 3 shows typical arrangement of reinforcement and Fig. 4 shows the provided reinforcement in the test span (middle 1200 mm) and outside the test span. The reinforcement in the test span was calculated based on the applied loads while more longitudinal and transverse steel was provided outside the test span to resist negative

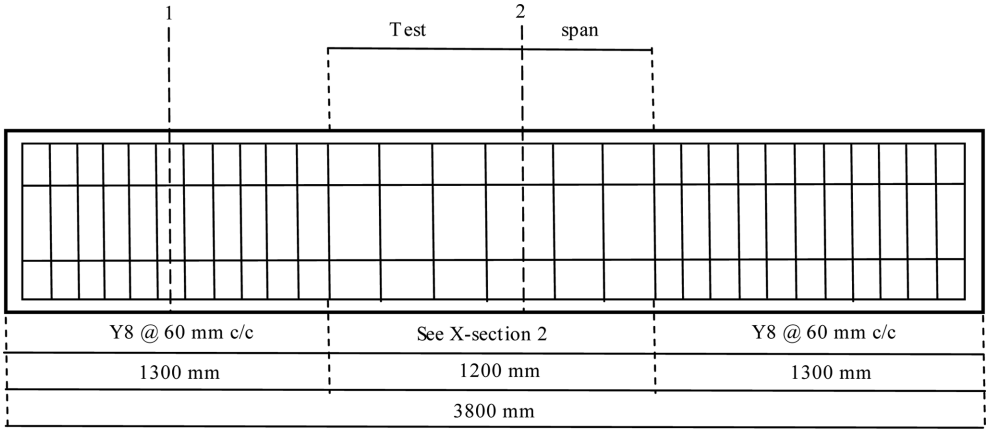

Fig. 3 Typical arrangement of reinforcement

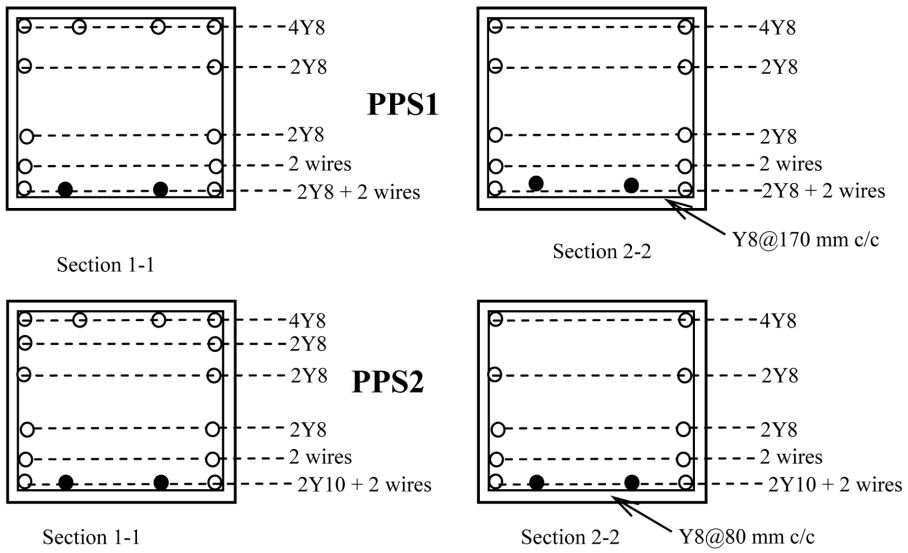

Fig. 4 Provided reinforcement

moment at the supports and to ensure failure occurred in the test span.

The formwork was made of a wooden box while the tensioning rig was made up of longitudinal and transverse hollow steel sections. The pre-stressing wires were tensioned using a simple arrangement of two nuts with ball bearings such that the wire could be stressed with a pair of spanners by tightening the nuts. The force in the wires was measured using a simple load cell developed for this purpose.

Three concrete cubes ($150 \times 150 \times 150$ mm) and three cylinders (150×300 mm) were cast for each beam from the concrete used for the beam.

8.3 Instrumentation and testing procedure

The beam was simply supported and was subjected to a mid-span concentrated load to generate

bending moment and shear force. Twisting moment was applied through twisting arms clamped at the ends. Fig. 5 shows typical load and support arrangement. This support and loading arrangements allowed free rotation about a longitudinal axis below the soffit of the beam as well as displacement in the beam axial direction and pin action.

6 mm long strain gauges, were used to measure the strain in the prestressing wires and the transverse reinforcement. The solid circles in Fig. 4 represent the pre-stressing wires which were strain gauged while the hollow circles represent the un-instrumented ones. The strain gauges in the stirrups were fixed at mid-depth. A legend for the strain gauges and their locations are shown in

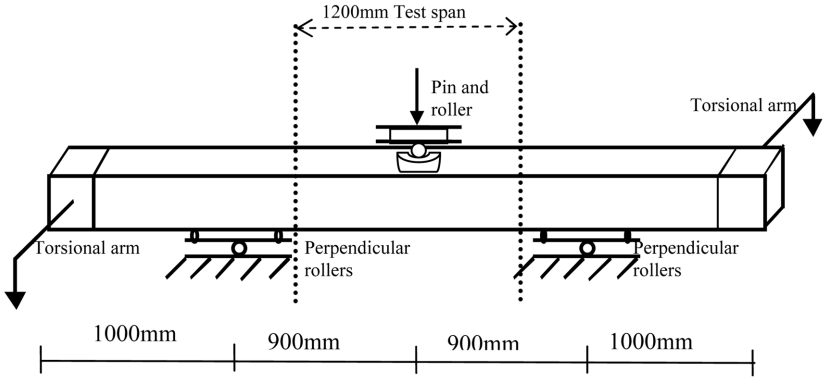

Fig. 5 Typical load and support arrangement

Table 3 Location of strain gauges (To be read in conjunction with Fig. 6)

Space	*a*	*b*	*c*	*d*	*e*	*f*	*g*
Beam	mm	mm	mm	mm	mm	mm	mm
PPS1	170	170	-	85	170	170	170
PPS2	80	80	80	40	80	80	80

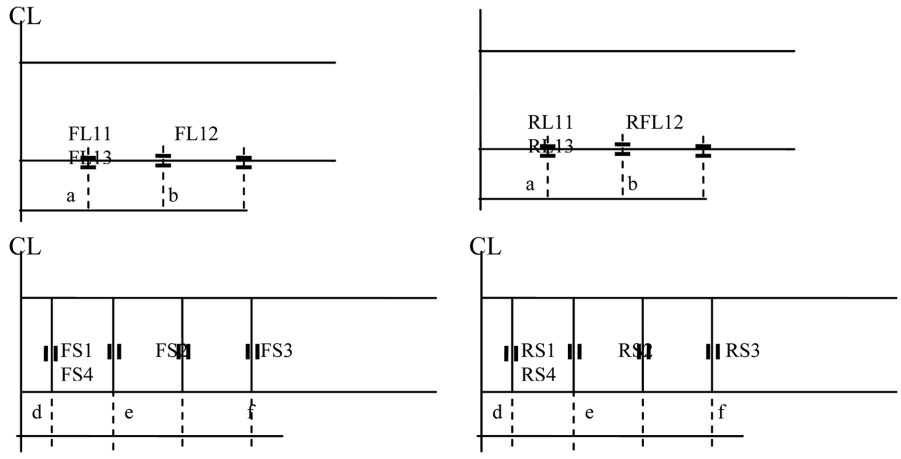

Fig. 6 Legend for strain gauge locations (to be read in conjunction of Table 3)

Table 3 and in Fig. 6. In Fig. 6, the first letter denotes side (F = Front side, R = rear side), the second letter denotes the type of reinforcement (L = Longitudinal, S = Stirrup), the first numeral in the longitudinal steel denotes the layer level (1 = the bottom layer) and the numeral in the stirrup and the second numeral in the longitudinal steel represent the horizontal location (1 = closest to mid-span). For example, FL12 = Front side, Longitudinal pre-stressing wire, at the bottom layer and at the second location from the mid-span and RS1 = rear side, Stirrup, at the first location from the mid-span. Only, the wires and transverse reinforcement in the 600 mm region to the right of mid-span were strain gauged. In this region the shear stresses are added in the front side and subtracted in the rear side.

For the measurement of twist, 3 Linear Variable Differential Transducers (LVDT) were used on the centreline of the front and rear faces as shown in Figs. 7(a),(b). Rotation at any of the vertical sections was obtained by dividing the vertical difference in displacement between directly opposite transducers by the distance between these points as shown in Fig. 8(a). Using the notations in this figure the angle of twist is equal to $(d_r + d_f)/L_h$. In the tested beams, the relative twist is the difference between the angle of twist θ_2 caused by the displacements in transducers 3 and 6 (Fig. 7) and the angle of twist θ_1 caused by the displacements in transducers 1 and 4. The rate of twist $\omega = (\theta_2 - \theta_1)/r$, where r is the distance between the two sections (Fig. 8(b)).

Linear Variable Differential Transducers (LVDT) were used to measure the beam deflection at mid-span. All strain gauges and LVDTs were connected to a data logger.

The crack widths were measured using a crack width measuring microscope.

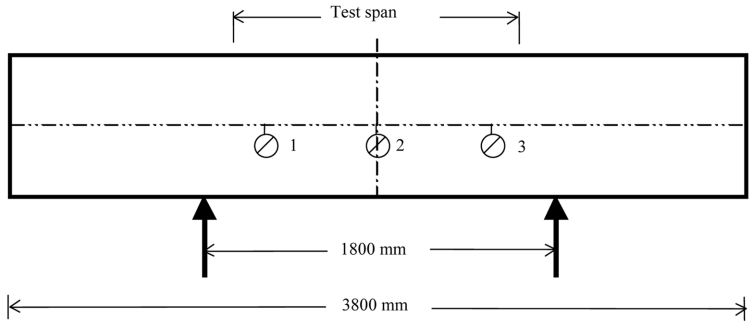

(a) LVDT at the front face

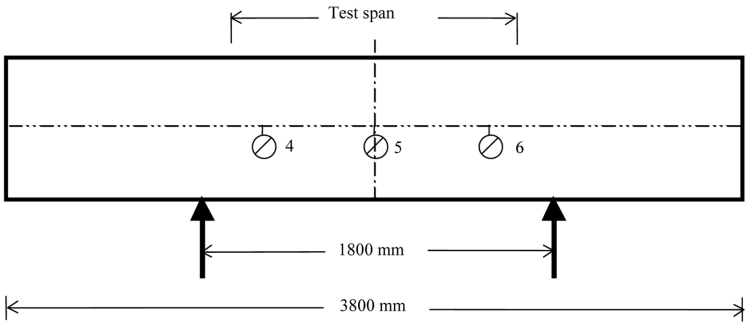

(b) LVDT at the rear face

Fig. 7 Location of transducers

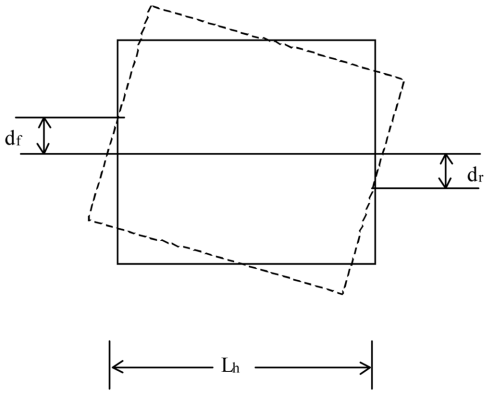

(a) Angle of twist at a section $\theta_t = (d_f+d_r)/L_h$

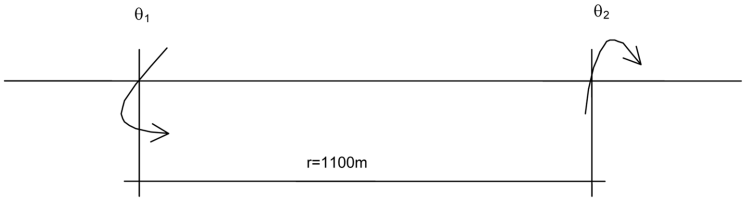

(b) Rate of twist $\omega = (\theta_2 - \theta_1)/r$

Fig. 8 Deformation of beam section due to torsion

Table 4 Average material properties

Beam No.	f_{cu}	f_c'	f_y	f_{yv}	f_{pu}	f_{py}	f_{pe}
	N/mm²	N/mm²	N/mm²	N/mm²	N/mm²	N/mm²	N/mm²
PPS1	52	36	500	500	1670	1570	1018.6
PPS2	53	36	500	500	1670	1570	1018.6

For each experiment, the design load was divided into load increments. The value of each of the first three increments was 10% of the design load (10% torsion + 10% bending moment) while for each of the rest increments it was 5% of the design load until failure. The beam was considered to have collapsed when it could resist no more loads. This usually happened after major crack(s) propagate(s) around the beam cross-section near the mid-span dividing the beam into two parts connected by the longitudinal reinforcement.

The beam and its associated cubes and cylinders were tested on the same day. Table 4 shows the average measured material properties. The concrete cube and cylinder compressive strengths shown in this table are the average strengths that were obtained from samples cured along side each beam.

8.4 Experimental observations

This section summarises the observed behaviour in the test span region at significant behaviour

stages. The crack direction angle was measured relative to the horizontal axis. Vertical displacement was measured at mid-span and in the bottom face. Strain ratios in the bottom layer of the pre-stressed wires and in the transverse steel in the test span are presented. The quoted load factor is the experimentally measured load at each increment expressed as a percentage of the design load, L.F. = $(M_i/M_d + T_i/T_d)/2$ including the self-weight. The failure load is the experimentally measured failure load as a percentage of the design load, $L_e/L_d = (M_e/M_d + T_e/T_d)/2$.

The average strain ratio in the wires $\varepsilon/\varepsilon_{yp}$ is the average of the measured strain at each load increment to the yield strain of the wires. The average strain ratio in the stirrups $\varepsilon/\varepsilon_{yv}$ at each load increment is the average of the measured strain to the yield strain of the stirrups. At each strain gauge location on the wires or the stirrups, the average of the readings from the two opposite strain gauges is used.

PPS1: T_d = 13 kNm, M_d = 50.89 kNm, V_d = 61.08 kN, T_d/M_d = 0.26, τ_{tor}/τ_{shr} = 0.69

At 70% of design load, almost vertical cracks were first noticed in the front, rear and bottom faces near mid-span. Displacement limit of span/250 was reached at 80% of load. From 80% to 110% of load, inclined cracks developed in these three faces. The average crack width at 110% of load was 0.4 mm. At 120% of load, a major crack opened up in the front and bottom faces about 200 mm to the right of mid-span and immediately extended into the rear and top faces spiralling round the beam section causing failure as shown in Fig. 9. Fig. 10 shows the maximum observed vertical displacement at mid-span. The jump in displacement between the values 1.75 mm and 10.46 mm is assumed to be an outlier and modified values are plotted as shown. Fig. 11 shows the relative angle of twist with minimal values until about 70% of the design load. Figs. 12-15 show the strain ratios in the pre-stressing wires and the transverse steel. The average strain ratio in the front

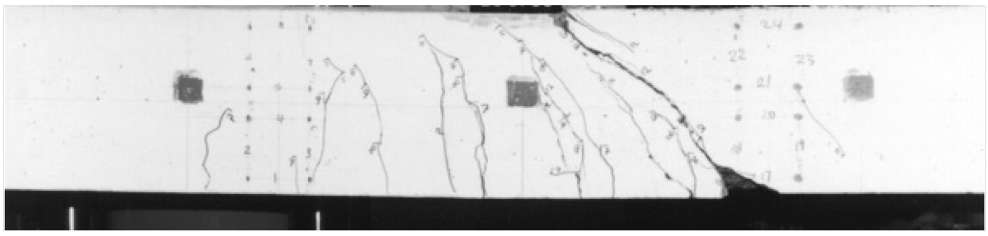

Fig. 9 Crack development in the front face (PPS1)

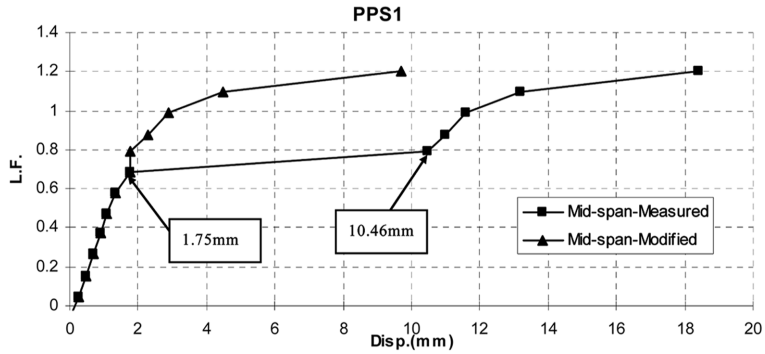

Fig. 10 Vertical displacement at mid-span (PPS1)

side wire was 1.34 and in the rear side wire was 1.2. In the stirrups, the average strain ratio in the front face was 0.43 and in the rear face was 0.13.

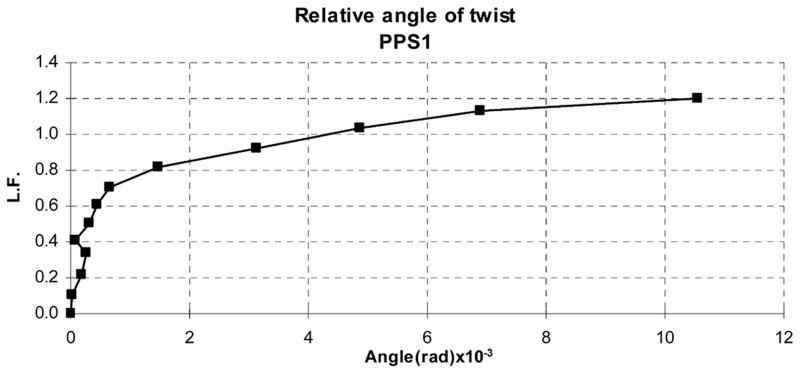

Fig. 11 Relative angle of twist (PPS1)

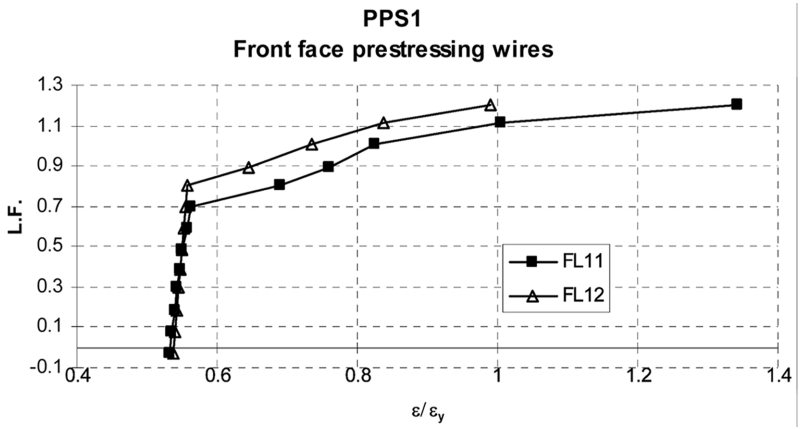

Fig. 12 Strain ratios in the front face pre-stressing wires (PPS1)

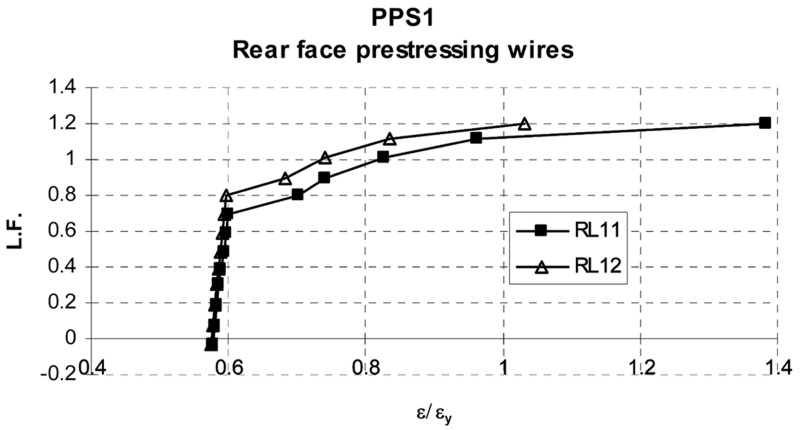

Fig. 13 Strain ratios in the rear face pre-stressing wires (PPS1)

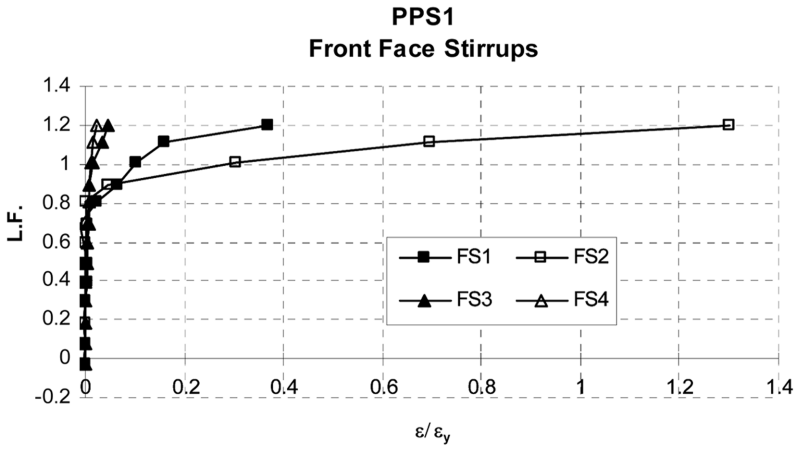

Fig. 14 Strain ratios in the front face stirrups (PPS1)

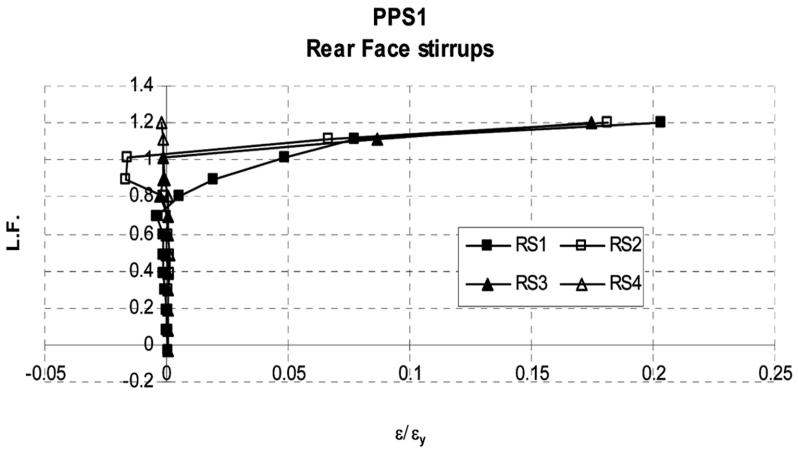

Fig. 15 Strain ratios in the rear face stirrups (PPS1)

PPS2: T_d = 39 kNm, M_d = 32.89 kNm, V_d = 41.08 kN, T_d/M_d = 1.19, τ_{tor}/τ_{shr} = 3.04

Inclined (50°) cracks appeared on all faces at 50% of design load. With an increase of load, more cracks developed until failure happened at 97% of load by several cracks opening up in the bottom, rear and top faces as shown in Fig. 16. The average crack width before failure load was 0.4 mm.

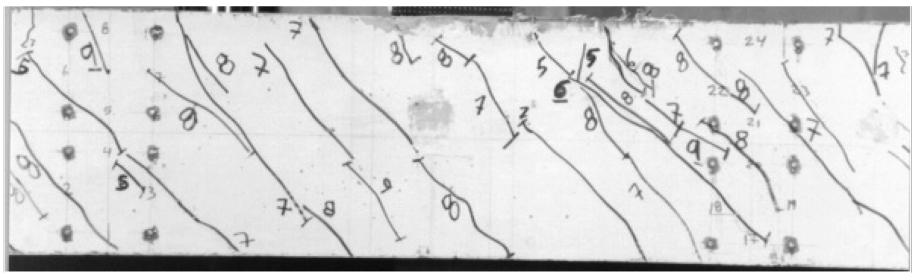

Fig. 16 Crack development in the front face (PPS2)

Fig. 17 shows that the maximum observed vertical displacement at mid-span were very small with exception to the last reading. Fig. 18 shows the relative angle of twist with minimal values until about 45% of the design load. Figs. 19-22 show strain ratios in the pre-stressing wires and transverse steel. It is clear that most of the longitudinal wires and front face stirrups yielded or

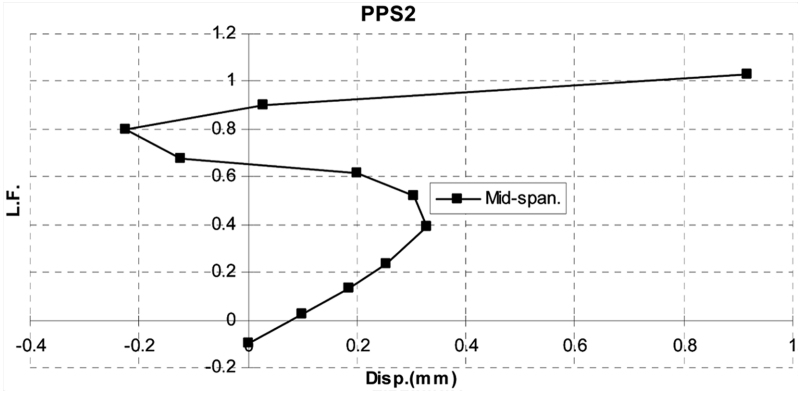

Fig. 17 Vertical displacement at mid-span (PPS2)

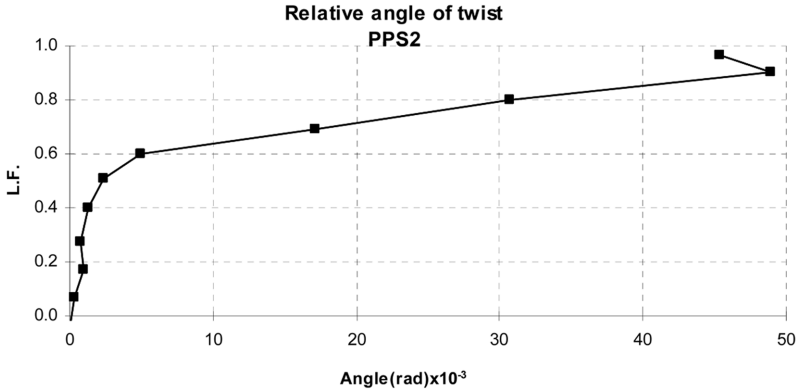

Fig. 18 Relative angle of twist (PPS2)

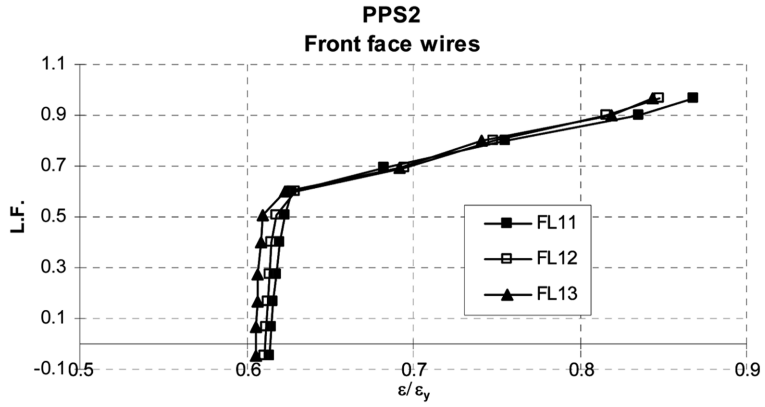

Fig. 19 Strain ratios in the front face pre-stressing wires (PPS2)

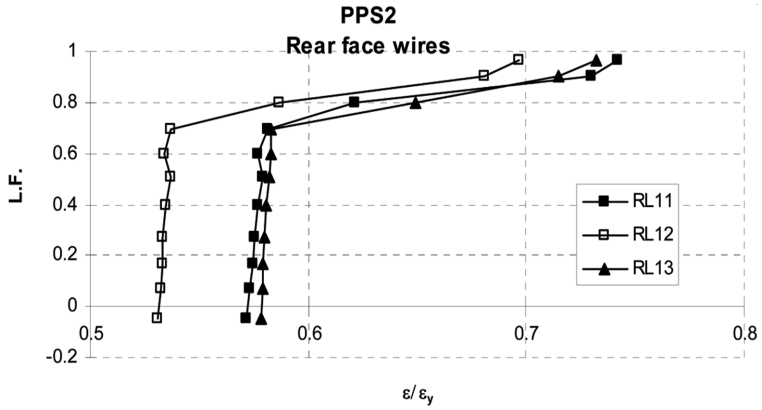

Fig. 20 Strain ratios in the rear face pre-stressing wires (PPS2)

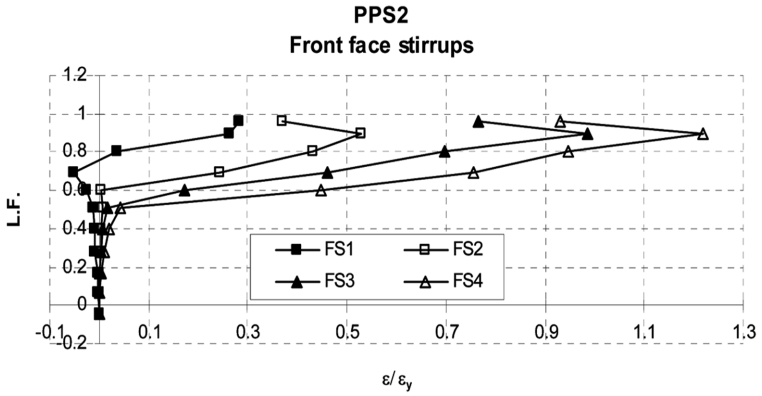

Fig. 21 Strain ratios in the front face stirrups (PPS2)

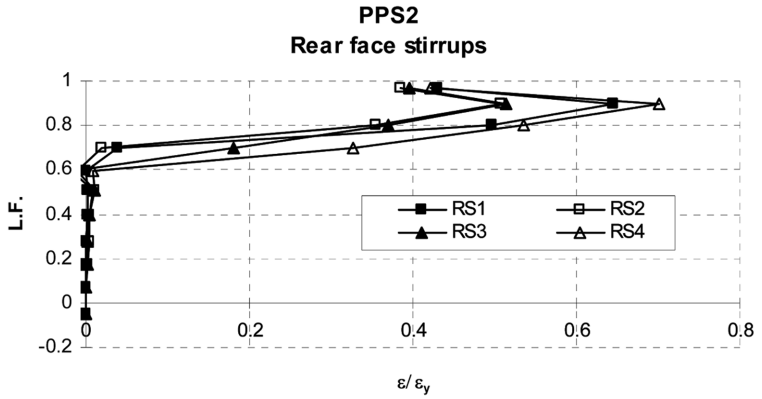

Fig. 22 Strain ratios in the rear face stirrups (PPS2)

reached near yield strain. The average strain ratio in the front side wire was 0.85 and in the rear side wire was 0.71. In the stirrups, the average strain ratio in the front face was 0.59 and in the rear face was 0.41.

9. Discussion of results

From the experimental results, the following general points can be highlighted:

1) From the results in Table 5 it can be seen that lower ratios of T_d/M_d and τ_{tor}/τ_{shr} (PPS1, bending dominance) leads to measured failure load larger than the design load. This can be due to confinement that large compressive normal stress causes in the concrete which allows utilization of tension steel in the hardening stage and lead to higher failure load. When the torsion was dominant, PPS2, the measured failure load was close to the design load.
2) It is clear from Table 6 that when $T_d/M_d > 1$ the cracks started earlier than when $T_d/M_d < 1$. In addition, the 0.3 mm crack width was reached at load ratio larger when bending was dominant than when torsion was dominant. This might be due to the fact that at the side where shear stresses are added the cracks start earlier and become wider due to the pronounce effect of torsion.
3) Figs. 10 and 17 show that beam PPS1 underwent much larger displacement than beam PPS2, possibly because beam PPS1 was subjected to a larger vertical load and behaved in a more ductile manner than beam PPS2.
4) The effect of torsion is clear in producing large maximum angle of twist in beam PPS2 than in beam PPS1 as shown in Figs. 11 and 18. PPS1 had very small values for the angle of twist (linear) until about 70% of the design load while beam PPS2 started the nonlinearity at an earlier load (45%).
5) In beam PPS1, the first yields in the pre-stressed wires and the stirrups were recorded in front face at about 1.2 of the design load (Table 6). However, in beam PPS2 which had a large T_d/M_d ratio, the wires reached less than 90% of yield strain. This is due to the larger bending moment that was resisted by beam PPS1 than PPS2. The first yield strain was reached in the front face stirrups in PPS2 at load ratio of 80% while in PPS1 the first yield in the stirrups was reached at 1.2 of the design load. This is to be expected since the shear stresses due to large torsion (in the case of PPS2) and due to the shear force are added on the front side.

Table 5 Failure load ratios

Load	τ_{tor}/τ_{shr}	T_d/M_d	L_e/L_d	L_c/L_d	L_eL_c
Beam	Ratio	Ratio	Ratio	Ratio	Ratio
PPS1	0.69	0.26	1.2	1.2	1.00
PPS2	3.04	1.19	0.97	0.95	1.02
	Average		0.995	1.075	1.01

Table 6 Test results related to crack, displacement and steel strain

Beam No.	Load at first crack	Load when crack width was 0.3 mm	Δ	First yield data				Max. steel strain measured data			
				FYL	LFL	FYS	LFS	$(\varepsilon/\varepsilon_{py})$MFL	MFL	$(\varepsilon/\varepsilon_{yv})$MFS	MFS
	Ratio	Ratio	mm								
PPS1	0.7	0.9	9.7	FL11	1.2	FS2	1.2	1.4	FL11	1.3	FS2
PPS2	0.5	0.8	0.9	-	-	FS4	0.8	0.86	FL11	1.2	FS4

6) In both beams, the rear side stirrups did not reach yield due to the fact that for practical reasons the beam was over-reinforced in the transverse rear side as the stirrups used were based on the required front side steel where the shear stresses are added. Nevertheless, as can be seen from Figs. 17 and 22 that the larger the T_d/M_d ratio the larger the strain ratio.
7) In the case of beam PPS1 in which bending was dominant ($T_d/M_d < 1$) almost vertical cracks started at the bottom face and near the bottom of the front and rear sides. These cracks were followed by inclined cracks at succeeding load increments until they first appeared in the top face. In beam PPS2 where torsion was dominant ($T_d/M_d > 1$), inclined cracks extended into the bottom face after they were formed in the front and rear sides. This is due to the fact that the largest shear stress is located at mid-depth of front face where the shear stress due to shear force is maximum and added to a large torsional shear stress in beam PPS2. In general, the smaller the ratios T_d/M_d, the closer are the cracks to vertical. The number of cracks was more in the case of torsion dominant beam (PPS2) than in the bending dominant beam (PPS1).
8) In both beams, it was found that vertical cracks occur near mid-span in the bottom face and in the lower half of the front and rear sides while the inclined cracks occur all along the length of the beam. This is because torsion was constant throughout the entire length while the maximum bending moment was located in middle of the beam.
9) In beam PPS1 the mode of failure was flexural where the beam experienced relatively large displacement and the flexural steel yielded. A small number of cracks caused failure at the time of flexural steel yielding. Beam PPS2 failed by diagonal cracking due to high torsional shear stress and the failure mode was less ductile with small displacement, less wire strain and larger transverse steel strain than beam PPS1. This clearly reflects the effect of torsion on the concentration of shear stress in the periphery of the cross-section.

10. Conclusions

From the results shown in this paper, it can be concluded that the direct design method produces a safe design for partially prestressed concrete solid beams under combined bending, shear and torsion loading. Both beams tested in this research failed within an acceptable range of the design loads (97-120%) and underwent ductile behaviour towards failure. Large variations in the design load combinations (i.e. T_d/M_d from 0.26 to 1.19 and τ_{tor}/τ_{shr} from 0.69 to 3.04) did not result in large differences in the experimental results. However, it was found that the higher the ratio T_d/M_d and the ratio τ_{tor}/τ_{shr} the lower the failure load. It was also found that when $T_d/M_d > 1$ the cracks started earlier in load ratio and the angle of twist was larger than when $T_d/M_d < 1$. The direct design procedure leads to the provision of reinforcement close to the ACI code but much less than the BSI code especially for transverse reinforcement. This means that the BSI code design equations for shear are conservative.

References

Abdel-Hafez Laila M. (1986), Direct Design of Reinforced Concrete Skew Slab, PhD thesis, University of Glasgow.
ACI Committee 318M (2002), Building Code Requirements for Structural Concrete (ACI 318M-02), Metric

version, American Concrete Institute, Farmington Hills, MI, 48333-9094, USA.
Aguilar, G., Matamoros, A.B., Parra-Montesinos, G.J., Ramraz, J.A. and Wight, J.K. (2002), "Experimental evaluation of design procedures for shear strength of deep reinforced concrete beams", *ACI Struct. J.*, **99**(4), 539-548.
Alnuaimi, A.S. and Bhatt, P. (2004a), "Direct design of hollow reinforced concrete beams-Part I: Design procedure", *Struct. Con. J.*, **5**(4), 139-146.
Alnuaimi, A.S. and Bhatt, P. (2004b), "Direct design of hollow reinforced concrete beams-Part II: Experimental investigation", *Struct. Con. J.*, **5**(4), 147-160.
Alnuaimi, A.S. and Bhatt, P. (2006a), "Direct design of partially prestressed concrete hollow beams", *Adv. Struct. Eng.*, **9**(4), 459-476.
Alnuaimi, A.S. and Bhatt, P. (2006b) "Design of reinforced concrete solid beams", *Struct. Buil. J., Thomas Telford Limited*, **159**(4), 197-216.
Alnuaimi, A.S., Al-Jabri, K.S. and Hago, A.W. (2007a), "Direct design of T-beams for combined load of bending and torsion", *J. Eng. Res.*, **4**(1), 23-35.
Alnuaimi, A.S., Al-Jabri, K.S. and Hago, A.W. (2007b), "Comparison between solid and hollow reinforced concrete beams", *Mater. Struct. J.*, (in press).
American Association for State Highway and Transportation Officials (1998), AASHTO LRFD Bridge Design specifications and Commentary, SI Units, Second Edition, Washington, D.C., pp.1091.
Bhatt, P. and Bensalem, A. (1996a), "Behaviour of reinforced concrete flat slab over column support using nonlinear stress field design", *Struct. Eng. Rev.*, **8**(2-3), 201-212.
Bhatt, P. and Bensalem, A. (1996b), "Use of non-elastic stress in the design of reinforced concrete deep beams", *Struct. Eng. Rev.*, **8**(2-3), 213-225.
Bhatt, P. and Ebireri, J.O. (1989), "Direct design of beams for combined bending and torsion", Stavebnicky Casopis, Building Journal (Bratislava), **37**(4), 249-263, in English, ISSN: 0039-078X, Coden: STVCA2.
Bhatt, P. and Mousa, J. (1996), "Tests on concrete box beams under non-monotonic loading", *Struct. Eng. Rev.*, **8**(2-3), 227-235.
BS8110 (1997), Structural Use of Concrete, Part 1: Code of Practice for Design and Construction, British Standard Institution, 389Chiswick High Road, London, W4 4AL.
Clark, L.A. (1976), "The provision of tension and compression reinforcement to resist in-plane forces", *Mag. Con. Res.*, **28**(94), 3-12.
Cohn, M.Z. and Lounis, Z. (1993), "Optimum limit design of continuous prestressed concrete beams", *J. Struct. Eng.*, **119**(12), 3551-3569.
CSA Standard, Design of Concrete Structures (A23.3-94) (1994), Canadian Standards Association, Rexdale, Ontario, Canada, 199.
Elarabi, H. (1999), "Application of the direct design method on reinforced concrete beams subjected to combined torsion, bending and shear", *Build. Road Res. J.*, University of Khartom, **2**, 47-56.
El-Hussein, E.A. (1994), "Finite element and direct design method in combined torsion, bending and shear of reinforced Concrete", Computational Structural Engineering for Practice, Civil-Comp Ltd., Edinburgh, Scotland, 165-171.
Hago, A. and Bhatt, P. (1986), "Tests on reinforced concrete slabs designed by direct design procedure", *ACI J.*, No. 83-79, 916-924.
Hsu, T.T. (1997), "ACI shear and torsion provisions for prestressed hollow girders", *ACI Struct. J.*, **94**(6), 787-799.
Hsu, T.T.C. (1968) "Torsion of structural concrete-behaviour of reinforced concrete rectangular members", SP-18, American Concrete Institute, Detroit, Michigan, 261-306.
Karayannis, C.G. and Chalioris, C.E. (2000), "Strength of prestressed concrete beams in torsion", *Struct. Eng. Mech.*, **10**(2), 165-180.
Kemp, K.O. (1971), "Optimum reinforcement in a concrete slab subjected to multiple loadings", *Publ. Int. Assoc. Bridge Struct. Eng.*, **31**, 93-105.
MacGregor, J.G. and Ghoneim, M.G. (1995), "Design for torsion", *ACI Struct. J.*, No. 92-S20, 211-218.
Memon, M. (1984), Strength and stiffness of shear wall-floor slab connections, PhD thesis, University of Glasgow.

Mitchell, D. and Collins, M.P. (1991), *Pre-stressed Concrete Structures*, Prentice Hall Inc., Englewood Cliffs, N.J.
Morley, C.T. and Gulvanessian, H. (1977), "Optimum reinforcement of concrete slab elements", *Proc. Ins. Civil Eng.*, Part 2, 63, June, 441-454.
Nielsen, M.P. (1974), "Optimum design of reinforced concrete shells and slabs", Structural Research Laboratory, Technical University of Denmark, Report NR.R44, pp.190-200.
Nielsen, T.B. (1985), "Optimization of reinforcement in shells, folded plates, walls and slabs", *ACI J.*, **82**(26), 304-309.
PCI Design Handbook (2004), "Pre-cast and prestressed concrete", Sixth edition, Pre-cast/Prestressed Concrete Institute, Chicago, IL.
Poulsen, P.N. and Damkilde, L. (2000), "Limit state analysis of reinforced concrete plates subjected to in-plane forces", *Int. J. Solids Struct.*, **37**(42), 6011-6029.
Rahal, K. and Collins, M.P. (1996), "Simple model for predicting torsional strength of reinforced and prestressed concrete sections", *ACI Struct. J.*, **93**(6), 658-666.
Rahal, K.N. (2001), "Analysis and design for torsion in reinforced and prestressed concrete beams", *Struct. Eng. Mech.*, **11**(6), 575-590.
Rahal, K.N. and Collins, M.P. (2003a), "Combined torsion and bending in reinforced and prestressed concrete beams", *ACI Struct. J.*, **100**(2), 157-165.
Rahal, K.N. and Collins, M.P. (2003b), "Experimental evaluation of ACI and ASHTO-LRFD design provisions for combined shear and torsion", *ACI Struct. J.*, **100**(3), 277-282.
Rahal, K.N. and Collins, M.P. (1995) "Analysis of sections subjected to combined shear and torsion – A theoretical model", *ACI Struct. J.*, **92**(4), 459-469.
Recupero, A., D'Aveni, A. and Ghesi, A. (2005), "Bending moment-shear force interaction domanins for prestressed concrete beams", *J. Struct. Eng.*, ASCE, **131**(9), 1413-1421.
Seraj, S.M., Kotsovos, M.D. and Pavlovic, M.N. (1993), "Compressive-force path and behaviour of prestressed concrete beams", *Mate. Struct.*, **26**(156), 74-89.
Thurlimann, B. (1979), "Torsional strength of reinforced and prestressed concrete beams-CEB approach". Institut fur Baustatik und konstruktion, ETH. Zurich., No.92, 117-143.
Wafa, F.F., Shihata, S.A., Ashour, S.A. and Akhtaruzzaman, A.A. (1995), "Prestressed high-strength concrete beams under torsion", *J. Struct. Eng.*, ASCE, **121**(9), 1280-1286.
Zia, P. and Hsu, T.T.C. (2004), "Design for torsion and shear in prestressed concrete flexural members", *PCI J.*, **49**(3), 34-42.

Appendix A

Design example

Calculate required reinforcement for a solid section to resist 13 kNm torsion T_d, 50.89 kNm bending moment M_d and 61.08 kN shear force V_d. The cross-section is 300 × 300 mm. The steel yield stress f_y for the longitudinal steel is 500 N/mm^2 and for the transverse steel f_{yv} is 500 N/mm^2. The concrete cube compressive strength f_{cu} is 52 N/mm^2 and the cylinder compressive strength f_c' is 36 N/mm^2. For pre-stressing, four 5 mm diameter wires were used in two locations as shown in Fig. A1(a). Each wire was stressed to a net force of P = 20 kN after losses. The eccentricity for the first group is e_1 =125 mm and for the second group is e_2 = 75 mm. The ultimate strength of the prestressing wires f_{pu} is 1670 N/mm^2, the yield strength of the wires f_{py} is 1570 N/mm^2 and effective stress after losses is f_{pe} = 1018.6 N/mm^2.

Solution:

The section is divided into 6 levels (a-f) and each level is divided into 6 regions (1-6) to give 36 cells as shown in Fig. A1(b).

$I = 6.75 \times 10^8$ mm^4

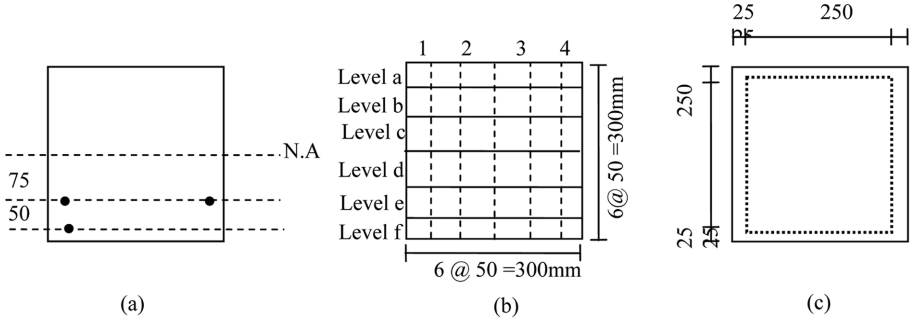

Fig. A1 Cross-section of solid beam: (a) Location of pre-stressing wires; (b) Cross-section of solid beam divided into 36 equal cells (c) centreline of shear flow

The torsional shear stress is assumed to be circulating in the outer 50 mm skin.
$A_o = 6.25 \times 10^4\ \text{mm}^2$ (area enclosed by the shear flow centreline, dotted line of Fig. A1(c))
$y_b = y_t = y = 150$ mm
$Z_b = Z_t = Z = I/y = 4.5 \times 10^6\ \text{mm}^3$

Normal stresses due to bending:

For elastic stress distribution, Eq. (A1) can be used (Fig. A2(a)).

$$\sigma_{xb} = \pm \frac{M_d y_i}{I} \tag{A1}$$

The results are presented in column 2 of Table A1 and apply to all regions at each level.

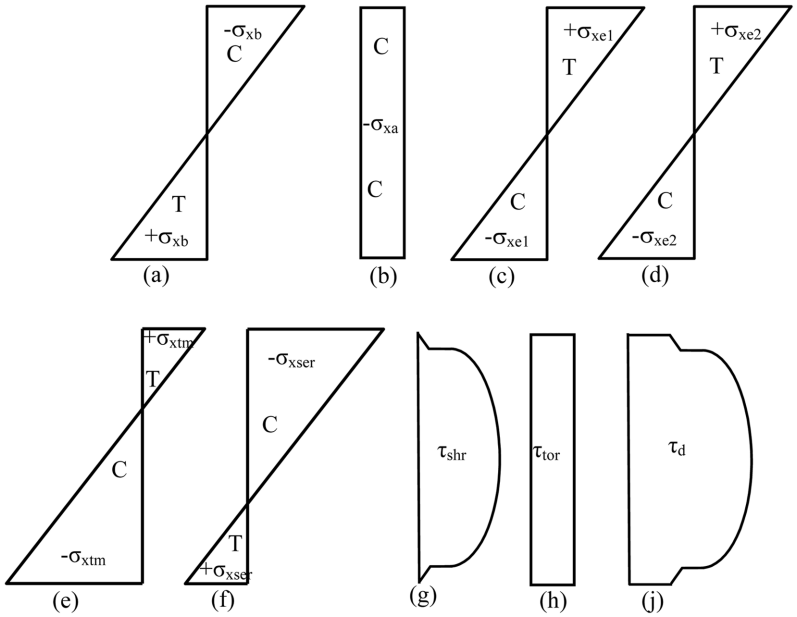

Fig. A2 Cross-section of the hollow beam: (a) normal stress due to bending, (b) normal stress due to axial load, (c) normal stress due to eccentricity 1, (d) normal stress due to eccentricity 2, (e) transfer normal stress, (f) service normal stress, (g) shear stress due to shear force, (h) shear stress due to torsion, (j) net shear stress where stresses for torsion and shear force are added

Table A1 Stress at the centroid of each level (N/mm^2)

1	2	3	4	5	6	7	8	9	10
Region	σ_{xb}	σ_{xa}	σ_{xe1}	σ_{xe2}	σ_{xtm}	σ_{xser}	σ_y	τ_{shr}	τ_{tor}
a	−9.42	−0.89	0.926	0.556	0.592	−8.83	0	~~0.28~~ =0	2.08
b	−5.65	−0.89	0.556	0.333	−0.001	−5.65	0	0.76	2.08
c	−1.88	−0.89	0.185	0.111	−0.594	−2.47	0	0.99	2.08
d	1.88	−0.89	−0.185	−0.111	−1.186	0.69	0	0.99	2.08
e	5.65	−0.89	−0.556	−0.333	−1.779	3.87	0	0.76	2.08
f	9.42	−0.89	−0.926	−0.556	−2.372	7.05	0	~~0.28~~ =0	2.08

Normal stresses due to pre-stressing:

Eq. (A2) can be used to calculate the normal stress due to axial load (Fig. A2(b)).

$$\sigma_{xa} = -\frac{P}{A_c} \tag{A2}$$

This is presented in column 3 of Table A1 and applies to all regions of each level.

Eq. (A3) can be used to calculate the normal stresses due to eccentricities (Fig. A2(c), (d)).

$$\sigma_{xe} = \pm\frac{P_i e_i}{Z} \tag{A3}$$

The results are shown in columns 4 and 5 of Table A1. Values at each level apply to all regions at that level.

The transfer normal stress σ_{xtm} (when only pre-stress forces act) is shown in column 6 of Table A1 (Fig. A2 (e)). The service normal stress σ_{xser} (when all service loads are applied) is given in column 7 of Table A1 (Fig. A2(f)). The service normal stress σ_{xser} is used in the design after checking that the compressive stresses in the top and bottom extreme fibres are not exceeding the allowable concrete compressive strength in both transfer and service conditions.

Since no out of plane bending is considered, $\sigma_y = 0$ at all regions (column 8 of Table A1).

Shear stresses due to shear force:

Eq. (A4) is used for the calculation of shear stresses due to shear force.

$$\tau_{shr} = \frac{V_d \int y_i d}{It} \tag{A4}$$

The result is shown in Column 9 of Table A1. It should be noted that the shear stress values in the top and bottom levels (a and f) are very small compared to the shear stresses in the middle levels (b, c, d, and e) and therefore can be ignored for design purposes.

Shear stresses due to torsion:

Shear flow is assumed to circulate in the outer 50 mm thick skin.

Eq. (A5) was used for the calculation of shear stress due to torsion. The result is shown in column 10 of Table A1. The values apply only to the outer cells and $\tau_{tor} = 0$ in the middle cells.

$$\tau_{tor} = \frac{T_d}{2tA_o} \tag{A5}$$

Combined shear stresses:

When the shear stresses due to shear force in the top and bottom levels (levels a and f) are ignored and the torsional shear stress is assumed to be limited to the outer 50 mm skin, the net shear stresses at each region are as shown in Table A2. It should be noted that in this table, the shear stresses in columns 1, 2 and 3 are

Table A2 Net shear stress distribution, τ, when top and bottom strips direct shear stress is ignored (N/mm^2)

Level	1	2	3	4	5	6
a	2.08	2.08	2.08	2.08	2.08	2.08
b	1.32	0.76	0.76	0.76	0.76	2.84
c	1.09	0.99	0.99	0.99	0.99	3.07
d	1.09	0.99	0.99	0.99	0.99	3.07
e	1.32	0.76	0.76	0.76	0.76	2.84
f	2.08	2.08	2.08	2.08	2.08	2.08

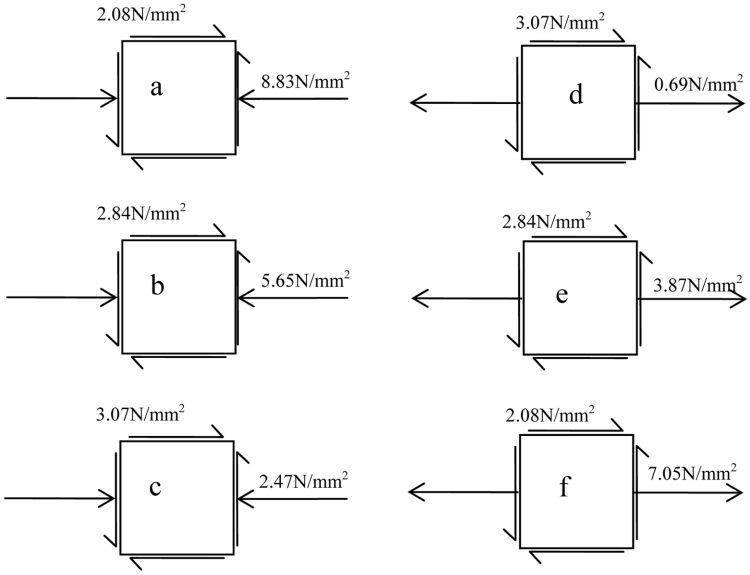

Fig. A3 Schematic representation of design normal and shear stresses

subtractive and in columns 4, 5 and 6 the shear stresses are additives.

Fig. A3 shows the directions of the net shear stresses. For practical reasons and due to the fact that torsional shear stresses exchange directions when crossing the beam centerline, the additive shear stresses were used in the design.

Fig. A4 shows a schematic representation of design normal and shear stresses. Table A3 shows the design shear stress distribution τ_d and Table A4 shows the ratios of total normal stress to the design shear stress, σ_{xser}/τ_d.

Calculation of forces per unit length and selection of design equations:

Table A5 shows the selections of Nielsen's design cases from Fig. A5 using ratios of $\sigma_{xser}/|\tau|$ in Table A4 and $\sigma_{y_i}/|\tau_d| = 0$.

Knowing that the width of each strip is 50 mm and using the equations from Fig. A5 the normal and transverse forces were calculated as shown in Tables A6 and A7 respectively. Tables A8 and A9 show the required reinforcement at each region in longitudinal and transverse directions respectively. It should be noted that the values in the last column of Table A9 are transverse reinforcement for one leg of the stirrup.

Note that in the cells were the prestressing wires are present the prestressing wires were assumed to act as unstressed steel with a yield stress equal to the difference between the yield stress f_{py} and the effective stress at service f_{pe} (Fig. A6) using the following equation

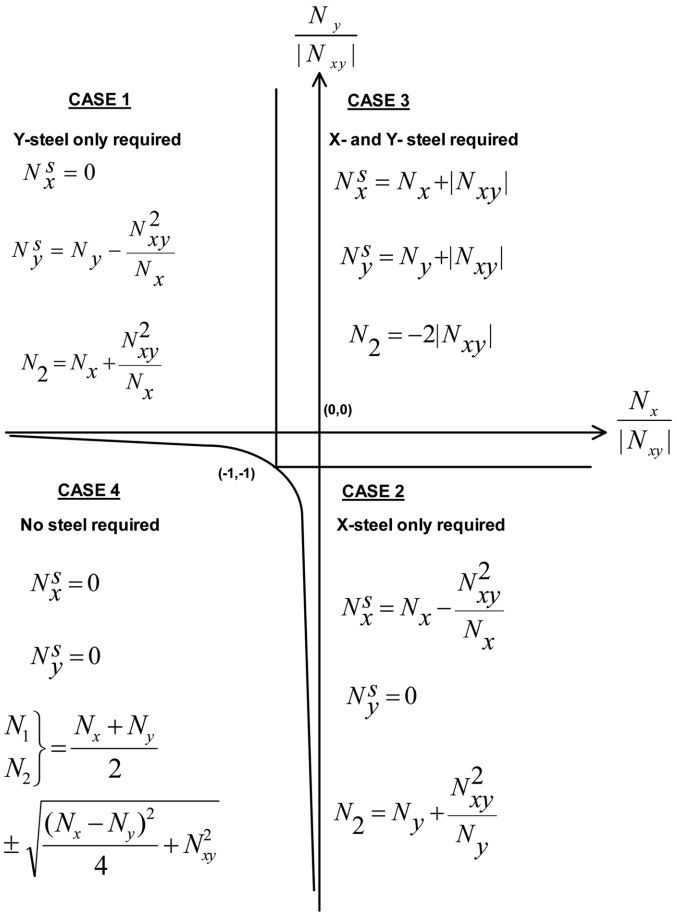

Fig. A4 Boundary graph for Nielsen's design equations

Table A3 Design shear stress distribution τ_d (N/mm^2)

Level	1	2	3	4	5	6
a	2.08	2.08	2.08	2.08	2.08	2.08
b	2.84	0.76	0.76	0.76	0.76	2.84
c	3.07	0.99	0.99	0.99	0.99	3.07
d	3.07	0.99	0.99	0.99	0.99	3.07
e	2.84	0.76	0.76	0.76	0.76	2.84
f	2.08	2.08	2.08	2.08	2.08	2.08

$$tN_x^s = A_s f_y + A_{sp}(f_{py} - f_{pe}) \quad \text{or}$$

$$A_s = \left[\left(N_x^s - \frac{A_{sp}}{t}(f_{py} - f_y)\right)/f_y\right]t$$

Table A4 Ratios of total normal stress to design shear stress σ_{xser}/τ_d

Level	1	2	3	4	5	6
a	−4.24	−4.24	−4.24	−4.24	−4.24	−4.24
b	−4.29	−7.39	−7.39	−7.39	−7.39	−1.99
c	−2.27	−2.50	−2.50	−2.50	−2.50	−0.81
d	0.64	0.70	0.70	0.70	0.70	0.23
e	2.94	5.06	5.06	5.06	5.06	1.36
f	3.38	3.38	3.38	3.38	3.38	3.38

Table A5 Selection of Nielsen's design case (use Table A6 and Fig. A4)

Level	1	2	3	4	5	6
a	1	1	1	1	1	1
b	1	1	1	1	1	1
c	1	1	1	1	1	3
d	3	3	3	3	3	3
e	3	3	3	3	3	3
f	3	3	3	3	3	3

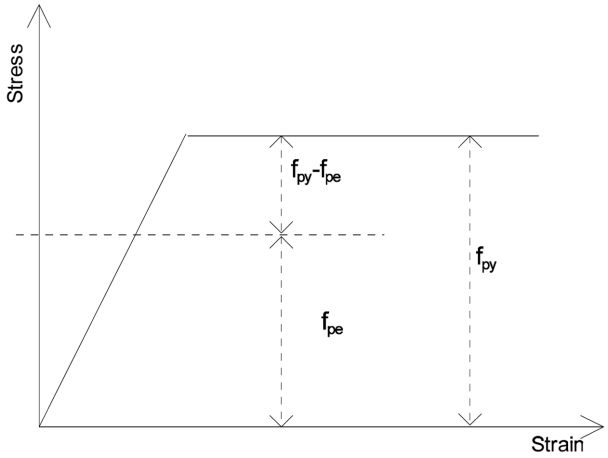

Fig. A5 Effective and yield stresses of pre-stressing wire

Table A6 Normal forces per unit length at each region, N_x^s (N/mm)

Level	1	2	3	4	5	6
a	0	0	0	0	0	0
b	0	0	0	0	0	0
c	0	0	0	0	0	29.8
d	89.3	84.3	84.3	84.3	84.3	188.3
e	259.2	231.5	231.5	231.5	231.5	335.5
f	455.9	455.9	455.9	455.9	455.9	455.9

Table A7 Transfer forces per unit length at each region, N_y^s (N/mm)

Level	1	2	3	4	5	6
a	24.5	24.5	24.5	24.5	24.5	24.5
b	71.6	5.2	5.2	5.2	5.2	71.6
c	190.4	19.8	19.8	19.8	19.8	190.4
d	153.5	49.5	49.5	49.5	49.5	153.5
e	142.2	38.2	38.2	38.2	38.2	142.2
f	104.0	104.0	104.0	104.0	104.0	104.0

Table A8 Required longitudinal reinforcement at each region, A_x (mm^2)

Level	1	2	3	4	5	6	Total at each level (mm^2)
a	0	0	0	0	0	0	0
b	0	0	0	0	0	0	0
c	0	0	0	0	0	3.0	3
d	8.9	8.4	8.4	8.4	8.4	18.8	61.3
e	−0.9	23.2	23.2	23.2	23.2	6.8	98.7
f	45.6	18.8	45.6	45.6	18.8	45.6	220
Total longitudinal reinforcement. mm^2							383

Table A9 Required transverse reinforcement at each level, A_y (mm^2/mm)

Level	1	2	3	4	5	6	Transverse reinforcement at each level (mm^2/m)
a	49.1	49.1	49.1	49.1	49.1	49.1	49.1
b	143.2	10.3	10.3	10.3	10.3	143.2	163.9
c	380.9	39.6	39.6	39.6	39.6	380.9	460.1
d	307.0	99.0	99.0	99.0	99.0	307.0	504.9
e	284.4	76.4	76.4	76.4	76.4	284.4	437.1
f	208.0	208.0	208.0	208.0	208.0	208.0	208.0
Transverse reinforcement used A_{sv} (mm^2/m)							504.9

Notation

N_x^s : steel resisting force in x direction
N_y^s : steel resisting force in y direction
$(A_s)_{ben}$: required unstressed reinforcement for bending
$(A_s)_{tor}$: required unstressed reinforcement for torsion
$(\varepsilon/\varepsilon_{py})$MFL : maximum strain ratios in front web pre-stressing wires
$(\varepsilon/\varepsilon_{yv})$MFS : maximum strain ratios in front web stirrups
Δ : maximum displacement at mid-span near failure load
a : depth of the equivalent rectangular block of the concrete compressive stress

$A_c = A_{cp}$: concrete cross-sectional area
$A_o = A_{oh}$: area enclosed by the centre line of the shear flow
A_s : required total unstressed reinforcement in the longitudinal direction
A_{sp} : Area of pre-stressing wires
A_{sv} : required area of two legs of a stirrup per meter (= A_v/S_v, mm^2/m)
b : breadth of the cross-section
d : distance from extreme compression fibre to centroid of tension reinforcement
E_c : Young's modulus of elasticity for concrete
e_j : eccentricities of the axial forces
f_c : concrete cylinder compressive strength
f_t' : concrete tensile strength
f_{cu} : concrete cube compressive strength
f_{pc} : compressive stress in concrete (after allowance for all pre-stress losses) at centroid of cross section resisting externally applied loads
f_{pe} : compressive stress in concrete due to effective prestress forces only (after allowance for all prestress losses) at extreme fibre of section where tensile stress is caused by externally applied loads
f_{pu} : ultimate strength of the pre-stressing wire
f_{py} : yield strength of the pre-stressing wire
f_y : yield strength of unstressed longitudinal steel
FYL, FYS : location of the first yield in the wires or stirrup respectively
f_{yv} : yield strength of transverse steel for shear (in our case $f_{yv} = f_{yt}$)
f_{yt} : yield strength of transverse steel for torsion (in our case $f_{yv} = f_{yt}$)
h : overall depth of cross section
I : moment of inertia of the cross-section
j : pre-stressing force reference
L.F. : load factor = $(T_i/T_d + M_i/M_d)/2$ at any load increment i
L_c/L_d : failure load ratio = $(T_c/T_d + M_c/M_d)/2$ for the last (failure) load increment
L_c/L_e : failure load ratio = $(T_c/T_e + M_c/M_e)/2$ for the last (failure) load increment
L_e/L_d : failure load ratio = $(T_e/T_d + M_e/M_d)/2$ for the last (failure) load increment
LFL, LFS : load factor at which first yield was recorded in a wire or stirrup respectively
MFL, MFS : location of maximum strain in front web wires and stirrups respectively
M_n : nominal bending moment strength
N_1 : concrete resisting force in the principle direction 1, (= $\sigma_1 t$)
N_2 : concrete resisting force in the principle direction 2, (= $\sigma_2 t$)
NR : not recorded
N_x : applied in-plane force per unit length in the x direction on a element with thickness t, (= $\sigma_{xser} t$)
N_{xy} : applied in-plane shear force per unit length on a element with thickness t, (= $\tau_{xy} t$)
N_y : applied in-plane force per unit length in the y direction on a element with thickness t, (= $\sigma_y t$)
P : total prestressing force in the section
p_h : perimeter of centreline of outermost closed transverse torsional reinforcement
P_j : individual axial forces in the pre-stressing wires after deducting all loses
p_{cp} : outside perimeter in the concrete cross-section
S_v : spacing between stirrups
t : thickness of the region (level)
T_d, M_d, V_d : factored design torsion, bending moment and shear force respectively
T_e, M_e : experimentally measured torsion and bending moment at failure
T_i, M_i : experimentally measured torsion and bending moment at load increment i
T_n : nominal torsional moment strength
V_c : ultimate shear resistance of the concrete
V_{co} : ultimate shear resistance of a section un-cracked in flexure
V_{cr} : shear resistance of a section cracked in flexure

M_o : moment necessary to produce zero stress at extreme tensile fibre which is a distance y from the centroid of the section
x_1 : the smaller centre-to-centre dimension of the rectangular link
y_1 : the larger centre-to-centre dimension of the rectangular link
$h_{\min}$: the smaller dimension of the beam section
$h_{\max}$: the larger dimension of the beam section
$(v_t)_{\min}$: minimum torsional shear stress of concrete, above which reinforcement is required
$(v_{tu})_{\max}$: ultimate torsional shear stress of concrete
v_c : nominal shear stress resistance of concrete
v_{shr} : shear stress due to applied shear force
v_{tor} : shear stress due to applied torsion
v : total shear stress due to applied shear force and torsion
w : width of region
y_b : distance between the centroidal axis and the extreme bottom fibre
y_i : distance between the centroid of the region i where the stress to be calculated and the neutral axis
y_t : distance between the centroidal axis and the extreme top fibre
Z : distance between the centroid of the longitudinal unstressed reinforcement and the centroid of the concrete compressive block
Z_b : elastic section modulus for the area below the centroidal axis ($= I/y_b$)
Z_p : distance between the centroid of the pre-stressing wires and the centroid of the concrete compressive block
Z_t : elastic section modulus for the area above the centroidal axis ($= I/y_t$)
σ_1 : concrete principle stress in direction 1
σ_2 : concrete principle stress in direction 2
σ_{xa} : applied normal stress due to axial load in the x direction
σ_{xb} : applied normal stress due to bending in the x direction
σ_{xe1} : applied normal stress due to eccentricity 1 of axial load 1 in the x direction
σ_{xe2} : applied normal stress due to eccentricity 2 of axial load 2 in the x direction
σ_{xser} : applied normal stress at service load ($= \sigma_{xb} + \sigma_{xser)}$
σ_{xstm} : applied normal stress at transfer ($= \sigma_{xa} + \sigma_{xe1} + \sigma_{xe2}$)
σ_y : applied normal stress in the y direction
ε : measured strain in the prestressed wires or stirrup as appropriate at any load increment i
ε_{py} : prestressed wires yield strain ($\varepsilon_{py} = f_{py}/E$)
ε_{yv} : transverse steel yield strain ($\varepsilon_{yv} = f_{yv}/E$)
τ_d : combined design shear stress due to torsion and shear force
τ_{shr} : applied shear stress due to shear force
τ_{tor} : applied shear stress due to torsion